

Band structure and gaps of triangular graphene superlattices

F. Guinea

Instituto de Ciencia de Materiales de Madrid. CSIC. Sor Juana Inés de la Cruz 3. 28049 Madrid. Spain

Tony Low

Hall for Discovery Learning Research, Purdue University, West Lafayette, IN47907-1791 Indiana, US

General properties of long wavelength triangular graphene superlattice are studied. It is shown that Dirac points with and without gaps can arise at a number of high symmetry points of the Brillouin Zone. The existence of gaps can lead to insulating behavior at commensurate fillings. Strain and magnetic superlattices are also discussed.

I. INTRODUCTION

Graphene is a two dimensional metal when carriers are induced by an electric field¹⁻⁴. A gap at the Fermi level has been observed by STM measurements^{5,6} (see also⁷). We analyze the gaps induced by a periodic structure, and the possibility that these gaps are generated spontaneously.

Graphene superlattices have been observed in graphene layers grown on transition metals^{8,9} (see also¹⁰⁻¹⁶). Superlattices are also found in graphene grown by the decomposition of SiC¹⁷. In general, graphene superlattices can have interesting properties, such as highly anisotropic transport properties¹⁸, or Dirac points at finite energies¹⁹⁻²³. In general, the study of the properties of graphene superlattices has attracted great interest, due to the many novel features their electronic spectra can show²⁴⁻³². In the following, we analyze general properties of the spectra of graphene superlattices with a two dimensional triangular periodicity. These superlattices share the symmetries of the graphene lattice, and are commonly found in graphene layers grown on metallic surfaces. As discussed below, these superlattices can show a gap at the Fermi energy for a number of commensurate fillings. It seems likely that they can be formed spontaneously on very uniform substrates, such as BNi, or due to intrinsic instabilities of graphene.

In this paper, we study the general properties of triangular graphene superlattices created by a scalar potential, followed by a discussion of strain and magnetic superlattices.

II. BRILLOUIN ZONE OF TRIANGULAR GRAPHENE SUPERLATTICES

We define the lattice vectors of the graphene lattice as:

$$\begin{aligned}\vec{a}_1 &\equiv \mathbf{n}_x \\ \vec{a}_2 &\equiv \frac{1}{2}\mathbf{n}_x + \frac{\sqrt{3}}{2}\mathbf{n}_y\end{aligned}\quad (1)$$

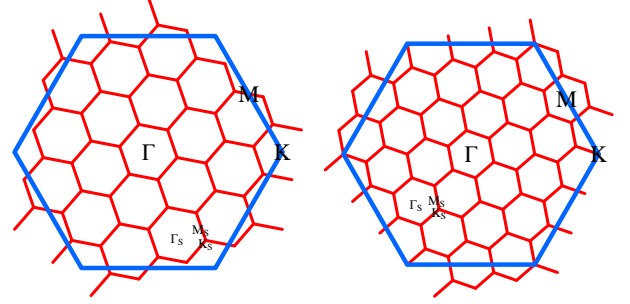


FIG. 1: (Color online). Examples of Brillouin Zones of superlattices. Left: $n_1 = 1, n_2 = 4$. Right: $n_1 = 2, n_2 = 4$.

A triangular superlattice is described by the unit vectors:

$$\begin{aligned}\vec{b}_1 &\equiv n_1\vec{a}_1 + n_2\vec{a}_2 \\ \vec{b}_2 &\equiv -n_2\vec{a}_1 + (n_1 + n_2)\vec{a}_2\end{aligned}\quad (2)$$

where n_1 and n_2 are arbitrary integers different from zero.

There are three types of high symmetry points in the Brillouin Zone of a triangular lattice, Γ , M and K . There are two inequivalent K points, K and K' , at the corners of the hexagonal Brillouin Zone, and three inequivalent M points, at the centers of the edges. Time reversal exchanges K and K' , while leaving the Γ point and the three M points unchanged³³. The vectors which define these points are such that:

$$\begin{aligned}\vec{\Gamma}\vec{a}_1 &= \vec{\Gamma}\vec{a}_2 = 0 \\ \vec{K}\vec{a}_1 &= \frac{4\pi}{3} \quad \vec{K}\vec{a}_2 = \frac{2\pi}{3} \\ \vec{K}'\vec{a}_1 &= \frac{2\pi}{3} \quad \vec{K}'\vec{a}_2 = \frac{4\pi}{3} \\ \vec{M}_1\vec{a}_1 &= \pi \quad \vec{M}_1\vec{a}_2 = \pi \\ \vec{M}_2\vec{a}_1 &= \pi \quad \vec{M}_2\vec{a}_2 = 0 \\ \vec{M}_3\vec{a}_1 &= 0 \quad \vec{M}_3\vec{a}_2 = \pi\end{aligned}\quad (3)$$

The low energy states of graphene lie close to the K and K' of the original Brillouin Zone. The positions of

these points in the superlattice Brillouin Zone is determined by:

$$\begin{aligned} \vec{K}_S \vec{b}_1 &= \frac{4\pi}{3}n_1 + \frac{2\pi}{3}n_2 & \vec{K}_S \vec{b}_2 &= -\frac{4\pi}{3}n_2 + \frac{2\pi}{3}(n_1 + n_2) \\ \vec{K}'_S \vec{b}_1 &= \frac{2\pi}{3}n_1 + \frac{4\pi}{3}n_2 & \vec{K}'_S \vec{b}_2 &= -\frac{2\pi}{3}n_2 + \frac{4\pi}{3}(n_1 + n_2) \end{aligned} \quad (4)$$

Thus, when $2n_1 + n_2$ is a multiple of three the graphene K and K' points will be mapped onto the Γ_S point of the superlattice Brillouin Zone. Otherwise, they will be mapped onto the corners of the Brillouin zone, K_S and K'_S . Examples of superlattice Brillouin Zones are given in Fig. 1.

III. DISPERSION NEAR HIGH SYMMETRY POINTS

A. The model

We study superlattices induced by a modulation of the on site energy of the π orbitals. We assume that it is a weak perturbation of the graphene Dirac equation, except in cases where degeneracies occur. We consider the Fourier components of the potential with lowest wavevector, of modulus:

$$G = \frac{4\pi}{a\sqrt{3(n_1^2 + n_2^2 + n_1n_2)}} \quad (5)$$

We write the potential as the sum of a symmetric part V_G , and an antisymmetric part, Δ_G , with respect to the interchange of sublattices. We neglect for the moment short wavelength components which mix the two inequivalent Dirac points of the unperturbed graphene layer.

We analyze the changes in the Fermi velocity near the Dirac energy induced by the superlattice potential, and the points in the lowest bands of the superlattice where degeneracies persist when $V_G \neq 0$ and $\Delta_G = 0$. As discussed below, this situation gives rise to a new set of Dirac equations at finite energies.

B. Dirac energy at the Γ_S point

We consider the case when the K and K' points of the graphene Brillouin Zone are mapped onto the Γ_S point of the superlattice Brillouin Zone. Using lowest order perturbation theory, we find, near the Γ_S point a renormalization of the Fermi velocity^{18,19}:

$$\delta v_F \approx -\frac{6|V_G|^2}{v_F G^2} + \frac{6|\Delta_G|^2}{v_F G^2} \quad (6)$$

There is a twofold degeneracy at the three M_S points, if $\Delta_G = 0$. The energy of these states is $v_F G/2$. At finite

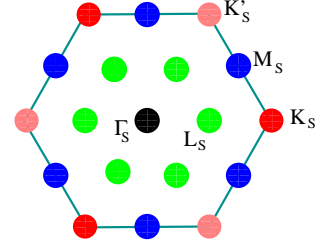


FIG. 2: (Color online). Points in the superlattice Brillouin Zone where degeneracies occur when $V_G \neq 0$.

distances from the M_S points, we can write an effective hamiltonian:

$$H \equiv \begin{pmatrix} \frac{v_F G}{2} + 2v_F k_x & \Delta_G + \frac{4iV_G k_y}{G} \\ \Delta_G - \frac{4iV_G k_y}{G} & \frac{v_F G}{2} - v_F k_x \end{pmatrix} \quad (7)$$

which gives an anisotropic Dirac equation with a gap:

$$\epsilon_{M_S} \approx \frac{v_F G}{2} \pm \sqrt{4v_F^2 k_x^2 + \Delta_G^2 + \frac{16V_G^2 k_y^2}{G^2}} \quad (8)$$

At the K_S and K'_S points, there are three degenerate levels for $V_G = \Delta_G = 0$, with energy $\epsilon_{K_S} = v_F G/\sqrt{3}$. When $V_G \neq 0$ these three levels are split into a doublet, with energy $\epsilon_{K_S}^d = v_F G/\sqrt{3} + V_G/2$, and a singlet, at $\epsilon_{K_S}^s = v_F G/\sqrt{3} - V_G$. Expanding around the K_S point, the effective hamiltonian for the doublet is:

$$H \equiv \begin{pmatrix} \frac{v_F G}{\sqrt{3}} + \frac{V_G}{2} - \frac{v_F k_x}{2} & \frac{v_F k_y}{2} - \frac{3i\Delta_G}{4} \\ \frac{v_F k_y}{2} + \frac{3i\Delta_G}{4} & \frac{v_F G}{\sqrt{3}} + \frac{V_G}{2} + \frac{v_F k_x}{2} \end{pmatrix} \quad (9)$$

This is the two dimensional Dirac equation with a mass term. The dispersion relation is:

$$\begin{aligned} \epsilon_{K_S}^s &\approx \frac{v_F G}{\sqrt{3}} - V_G + O\left(\frac{\Delta_G^2}{V_G}, \frac{v_F^2(k_x^2 + k_y^2)}{V_G}\right) \\ \epsilon_{K_S}^d &\approx \frac{v_F G}{\sqrt{3}} + \frac{V_G}{2} \pm \sqrt{\frac{v_F^2(k_x^2 + k_y^2)}{4} + \frac{9\Delta_G^2}{16}} \end{aligned} \quad (10)$$

There are two sets of degenerate bands, derived from the K and K' points of the Brillouin Zone of graphene. This degeneracy will be broken by short wavelength terms in the superlattice potential.

C. Dirac energy at the K_S and K'_S points

The renormalization of the Fermi velocity near the K_S and K'_S points is the same as in eq. 6.

There are doubly degenerate states, even when $V_G \neq 0$, at the six inequivalent points at positions $\vec{L}_S = \vec{K}_S/2$, as shown in Fig. 2. The energy of these points is

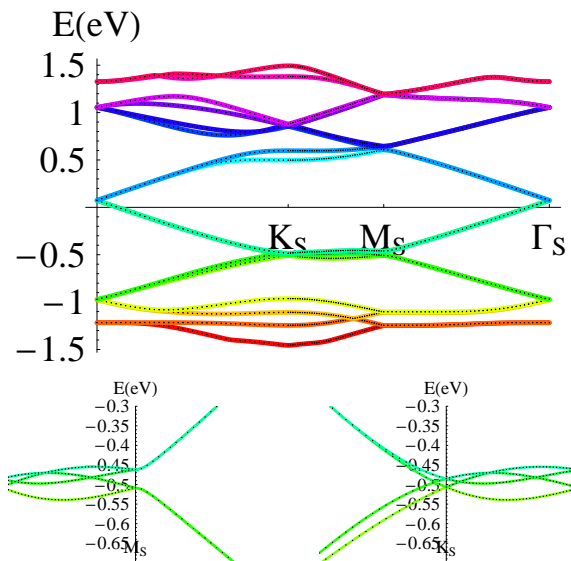


FIG. 3: (Color online). Top: Low energy bands for a 12×12 superlattice, with $V_G = 0.3\text{eV}$ and $\Delta_G = 0$. Bottom: Left: Details near the M_S point. Right: Detail near the K_S point.

$\epsilon_{L_S} = v_F G/2$. Expanding around these points, we find an effective anisotropic Dirac equation, given by eq.(7).

There are another set of doubly degenerate states at the M_S points. The two states arise from the K and K' points of the original graphene Brillouin Zone. The degeneracy persists when $V_G \neq 0$ and $\Delta_G \neq 0$, and is only broken by short wavelength components of the superlattice potential. When these components are finite, an effective anisotropic Dirac equation will arise similar to that in eq.(7).

For $V_G = \Delta_G = 0$ there are six degenerate states at the Γ_S point. The long range part of the superlattice potential will hybridize states which are derived from the K and K' points of the original graphene Brillouin Zone. We obtain two sets of isotropic Dirac equations, described by eq.(9), and two degenerate states. The short range part of the Dirac equation will break these degeneracies.

D. Results

We analyze the bands induced by a $N \times N$ superlattice. The hopping matrix between π orbitals in neighboring carbon atoms is $t = 3\text{eV}$. The bands for $V_G = 0.3\text{eV}$ and $\Delta_G = 0$ are shown in Fig. 3. The bands show Dirac points at the M_S and K_S points. When Δ_G is increased to $\Delta_G = 0.1\text{eV}$ a gap appears between successive bands, as shown in Fig. 4. The density of states for those two cases is shown in Fig. 5. Note that the potential breaks the electron-hole symmetry of clean graphene, and the gaps are not of the same magnitude for positive and negative energies.

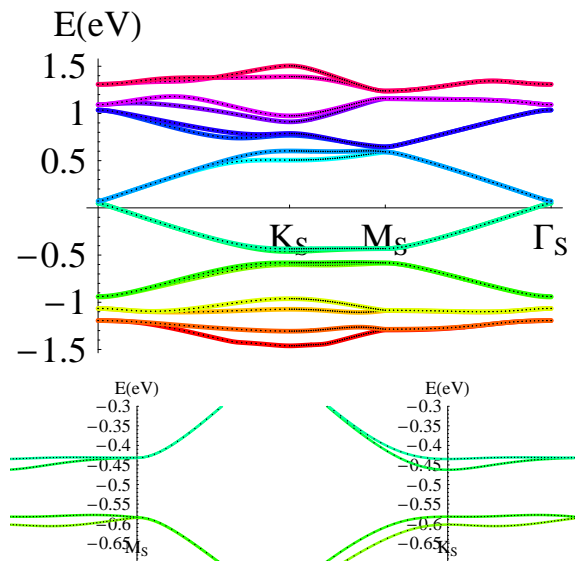


FIG. 4: (Color online). Top: Low energy bands for a 12×12 superlattice, with $V_G = 0.3\text{eV}$ and $\Delta_G = 0.1\text{eV}$. Bottom: Left: Details near the M_S point. Right: Detail near the K_S point.

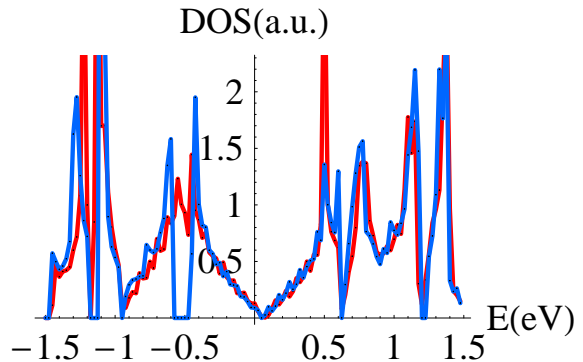


FIG. 5: (Color online). Density of states for a 12×12 superlattice. Red: $V_G = 0.3\text{eV}$ and $\Delta_G = 0$. Blue: $V_G = 0.3\text{eV}$ and $\Delta_G = 0.1\text{eV}$.

The results are in reasonable agreement with the analytical description in the previous section. A gap of order $2\Delta_G$ is induced at the M_S point. In order for this gap to be possible, the following inequalities must be satisfied:

$$\begin{aligned} \epsilon_{K_S}^s &\approx \frac{v_F G}{\sqrt{3}} - V_G \leq \epsilon_{M_S}^- \approx \frac{v_F G}{2} - \Delta_G \\ \epsilon_{M_S}^+ &\approx \frac{v_F G}{2} + \Delta_G \leq \epsilon_{K_S}^d \approx \frac{v_F G}{\sqrt{3}} + \frac{V_G}{2} - \frac{3\Delta_G}{4} \end{aligned} \quad (11)$$

The scaling properties of the Dirac equation imply that, if the dimension of the superlattice is increased, $G \rightarrow \lambda G$, with $\lambda < 1$, a rescaling of the superlattice potential, $V_G \rightarrow \lambda V_G, \Delta_G \rightarrow \lambda \Delta_G$, will lead to the same band structure, with energies scaled as $E \rightarrow \lambda E$.

IV. STRAIN SUPERLATTICES

A superlattice can also be produced by inducing strains, which modulate the interatomic hoppings. The corresponding perturbation can be seen as a gauge field, $\vec{\mathbf{A}}$, which shifts locally the momentum³⁴. A simple case

$$\begin{aligned} A_x(\vec{\mathbf{G}}) &= \frac{(\lambda + \mu)(G_x^2 - G_y^2) \left[h_{\vec{\mathbf{G}}}^{xx} G_y^2 - (h_{\vec{\mathbf{G}}}^{xy} + h_{\vec{\mathbf{G}}}^{yx}) G_x G_y + h_{\vec{\mathbf{G}}}^{yy} G_x^2 \right]}{|\vec{\mathbf{G}}|^4 (\lambda + 2\mu)} \\ A_y(\vec{\mathbf{G}}) &= \frac{(\lambda + \mu) 2G_x G_y \left[h_{\vec{\mathbf{G}}}^{xx} G_y^2 - (h_{\vec{\mathbf{G}}}^{xy} + h_{\vec{\mathbf{G}}}^{yx}) G_x G_y + h_{\vec{\mathbf{G}}}^{yy} G_x^2 \right]}{|\vec{\mathbf{G}}|^4 (\lambda + 2\mu)} \end{aligned} \quad (12)$$

where the tensor $h_{\vec{\mathbf{G}}}^{ij}$ is the Fourier transform of the functions:

$$h^{ij}(\vec{\mathbf{r}}) = \frac{\partial h}{\partial x_i} \frac{\partial h}{\partial x_j} \quad (13)$$

and λ and μ are the elastic Lamé coefficients of graphene. The field in eq. 12 has opposite signs in the two valleys in the Brillouin Zone.

The calculation of the effective magnetic field induced by the gauge field in eq. 12 is simplified when, as in the previous sections, only one component, $h(\vec{\mathbf{r}}) =$

is when the strains are due to height modulations, $h(\vec{\mathbf{r}})$, which can be induced by a substrate. In terms of the Fourier components of the modulation, $h_{\vec{\mathbf{G}}}$, and allowing for the relaxation of the in plane displacements, the effective gauge field can be written as³⁵:

$h_G \sum_{l=1, \dots, 6} e^{i\vec{\mathbf{G}}_l \vec{\mathbf{r}}}$, in a superlattice is considered. The tensor in eq. 13 has non zero components for all combinations of the type $\vec{\mathbf{G}}_k + \vec{\mathbf{G}}_l$. When the gauge field, $\vec{\mathbf{A}}(\vec{\mathbf{G}})$ is parallel to $\vec{\mathbf{G}}$, the vector potential can be gauged away, and does not induce an effective magnetic field. This implies that out of the 18 possible values of the vector $\vec{\mathbf{G}}_k + \vec{\mathbf{G}}_l$, only six contribute to the effective magnetic field. These vectors are given by $\vec{\mathbf{G}} \equiv G(3/2, \sqrt{3}/2)$ and the vectors equivalent to it by a symmetry transformation. After some algebra, we obtain for the effective magnetic field:

$$B_{strain}(\vec{\mathbf{r}}) = \frac{\beta}{a} \frac{\lambda + \mu}{\lambda + 2\mu} \frac{27\sqrt{3}}{8} G^3 h_G^2 \left[2 \cos(\sqrt{3}Gy) + 4 \cos\left(\frac{\sqrt{3}Gy}{2}\right) \left(\frac{3Gx}{2}\right) \right] \quad (14)$$

where $\beta = \partial \log(t) / \partial \log(a) \approx 2 - 3$, $t \approx 3\text{eV}$ is the nearest neighbor hopping, and $a \approx 1.4\text{\AA}$ is the distance between nearest neighbor carbon atoms. The superlattice defined by the effective magnetic field has a unit vector of length $\sqrt{3}G$, so that the area of its unit cell is a smaller than the area of the unit cell of the original superlattice by a factor 1/3.

Using eq. 14, and $G = 2\pi/L$, where L is the length of the unit vector of the superlattice, we can write the magnetic length associated to the maximum effective field in the system as:

$$\frac{1}{\ell_B^2} = \frac{\lambda + \mu}{\lambda + 2\mu} \frac{\beta}{a} \frac{9\sqrt{3}\pi^3}{2} \frac{h_{max}^2}{L^3} \quad (15)$$

where $h_{max} = 6h_G$ is the maximum value of $h(\vec{\mathbf{G}})$, assuming $h_G > 0$. For values $h_{max} \approx 1\text{nm}$, and $L \approx 40\text{nm}$, we find $l_B \approx 14\text{nm}$, so that the effective field is such that

$$B_{strain}^{max} \approx 1 - 2T.$$

V. MAGNETIC SUPERLATTICES

A superlattice can also be induced by a spatially modulated magnetic field. A combination of a modulated magnetic field and a scalar potential opens a gap at the Dirac energy, and the resulting insulator is a Quantum Hall system²⁴, with chiral currents at the boundaries³⁶. Here we obtain this effect using second order perturbation theory, instead of the arguments used in²⁴. As in the previous sections, we assume the simplest periodicity

compatible with the superlattice hexagonal symmetry

$$\begin{aligned} V(\vec{r}) &= V_G \sum_{l=1, \dots, 6} e^{i\vec{G}_l \vec{r}} \\ B(\vec{r}) &= B_G \sum_{l=1, \dots, 6} e^{i\vec{G}_l \vec{r}} \end{aligned} \quad (16)$$

The eigenstates of the unperturbed hamiltonian at the K and K' points of the Brillouin Zone can be written as $|0\rangle_A = (1, 0)$ and $|0\rangle_B = (0, 1)$, which each component of the spinor corresponds to one sublattice. These states are hybridized with states $|\vec{G}_\pm\rangle_K = (1, \pm e^{i\phi_{\vec{G}}})$ and $|\vec{G}_\pm\rangle_{K'} = (1, \mp e^{-i\phi_{\vec{G}}})$, with energies $\epsilon_{\vec{G}} = \pm v_F |\vec{G}|$, and $e^{i\phi_{\vec{G}}} = (G_x + iG_y)/|\vec{G}|$.

The energy of states $|0\rangle_A$ and $|0\rangle_B$ are modified in different ways by virtual hoppings into states $|\vec{G}_\pm\rangle_K$ and $|\vec{G}_\pm\rangle_{K'}$, leading to gaps in both valleys. Moreover, the gaps have different signs, showing that time reversal symmetry in the system is broken, and that a Quantum Hall phase has been induced. The gap can be written as

$$\Delta = \pm \sum_{l=1, \dots, 6} \frac{2v_F \text{Re} \left\{ V_{\vec{G}_l}^* \left[A_x(\vec{G}_l) + iA_y(\vec{G}_l) \right] e^{-i\phi_{\vec{G}_l}} \right\}}{|\epsilon_{\vec{G}_l}|} \quad (17)$$

where $\vec{A}_{\vec{G}}$ is the vector potential, which we define as:

$$\begin{aligned} A_x(\vec{G}) &= \frac{iG_y B_{\vec{G}}}{|\vec{G}|^2 \Phi_0} \\ A_y(\vec{G}) &= \frac{-iG_x B_{\vec{G}}}{|\vec{G}|^2 \Phi_0} \end{aligned} \quad (18)$$

where $\Phi_0 = eh/c$ is the quantum unit of flux. Using this expression, we finally obtain:

$$\Delta = 12 \frac{B_G V_G}{\Phi_0 G^2} \quad (19)$$

in agreement with²⁴.

VI. SELF CONSISTENT OPENING OF A GAP

The previous analysis shows that gap can open at finite energies in graphene in the presence of a superlattice potential with a staggered component. When the number of carriers is such that only a small number of subbands are completely filled and the rest are completely empty the electronic energy will be lowered in the presence of the gap. A lattice distortion which leads to the appropriate potential will be energetically favorable if the gain in electronic energy exceeds the formation energy of the distortion, as in the Peierls instability in one dimension.

In graphene on top of a metal or other substrate with a large dielectric constant, as in⁸, out of plane displacements lead to changes in the on site energies of the π

orbitals. An electron in a given carbon atom experiences the image potential due to the screening. A change of position of Δz leads to a change of the image potential of order $ee^* \Delta z / (4d^2)$, where $e^* = e(\epsilon_0 - 1)/(\epsilon_0 + 1)$ is the image charge, ϵ_0 is the dielectric constant of the substrate, and d is the distance to the substrate. A vertical displacement of $\Delta z \sim 1 \text{ \AA}$ when the graphene layer is at a distance $d \approx 3 \text{ \AA}$ of the substrate can lead to shifts of the onsite energies of order 0.1eV. The electronic gain of energy due to the existence of a gap, per unit cell, is then $E_{elec} \approx \Delta_G \approx ee^* \Delta z d^{-2}$.

The elastic energy per unit cell required to create a staggered distortion of amplitude Δz is of order $E_{elas} \approx \kappa \Delta z^2 a^{-2}$, where $\kappa \approx 1 \text{ eV}$ is the bending rigidity of graphene.

A gap will exist above a threshold for the superlattice potential, $V_G \sim \Delta_G \gtrsim v_F G (1/\sqrt{3} - 1/2)$. The area of the Brillouin Zone of the supercell, $\sqrt{3}G^2/2$ should be close to the area within the Fermi surface of the unperturbed graphene, πk_F^2 . Hence, a spontaneous staggered distortion is favored if:

$$\begin{aligned} E_{elec} + E_{elas} &\approx -\frac{ee^* \Delta z}{d^2} + \kappa \left(\frac{\Delta z}{a} \right)^2 < 0 \\ V_G &\approx \frac{ee^* \Delta z}{d^2} > v_F G \left(\frac{1}{\sqrt{3}} - \frac{1}{2} \right) \\ \frac{\sqrt{3}G^2}{2} &\approx \pi k_F^2 \end{aligned} \quad (20)$$

The last equation in (20) implies that $G \propto k_F$, and from the first two we obtain that $v_F G \lesssim (ee^*)^2 a^2 d^{-4} \kappa^{-1}$. Hence, a spontaneous distortion is energetically favored for carrier densities such that:

$$\rho = \pi k_F^2 \lesssim \frac{(ee^*)^4 a^4}{v_F^2 \kappa^2 d^8} \quad (21)$$

and the staggered distortion, with inverse wavelength $G \sim k_F$ of the order:

$$\Delta z \sim \frac{v_F k_F d^2}{ee^*} \quad (22)$$

For a metal, we have $e_0 = \infty$ and $e^* = e$. For $a \approx 2 \text{ \AA}$, $d \approx 3 \text{ \AA}$ and $\kappa \approx 1 \text{ eV}$, we find that a staggered corrugation is energetically favored for carrier densities $\rho \lesssim 10^{13} \text{ cm}^{-2}$, leading to maximum deformations of 0.2 \AA . For SiO_2 , where $\epsilon_0 = 3.9$ and $e^* \approx 0.6e$, the corrugations takes place for carrier densities $\rho \lesssim 3 \times 10^{12} \text{ cm}^{-2}$, and maximum deformations of 0.15 \AA .

The formation of these long wavelength modulations is only possible in systems with a high degree of order, as the superlattice features will be reduced by disorder. For instance, weak scatterers with concentration n_{imp} , which change the onsite potential by an amount of order Δ_G , lead to a mean free path $l_{el} \sim v_F^2 / (\Delta_G^2 k_F a^4 n_{imp})$. A large concentration of these defects, $n_{imp} \sim a^{-2}$ will suppress the formation of a superlattice, while affecting little the conductivity, $\sigma \sim (e^2/h) \times (k_F l_{el}) \sim (e^2/h) \times (v_F^2 a^{-2} \Delta_G^{-2})$.

VII. CONCLUSIONS

We have analyzed the formation of Dirac points and gaps at high energy points of triangular graphene superlattices. We have shown that in some cases a gap can be formed over the entire Fermi surface, making graphene insulating. We have discussed instabilities which might give rise to the spontaneous formation of gaps of this type. General properties of strain and magnetic superlattices are also discussed.

VIII. ACKNOWLEDGEMENTS

We appreciate useful conversations with J. L. Mañes, R. Miranda, and A. Vázquez de Praga. Funding from MICINN (Spain) through grants FIS2008-00124 and CONSOLIDER CSD2007-00010 is gratefully acknowledged. TL acknowledges funding from INDEX/NSF (US).

-
- ¹ K. S. Novoselov, A. K. Geim, S. V. Morozov, D. Jiang, Y. Zhang, S. V. Dubonos, I. V. Grigorieva, , and A. A. Firsov, *Science* **306**, 666 (2004).
- ² K. S. Novoselov, D. Jiang, F. Schedin, T. J. Booth, V. V. Khotkevich, S. V. Morozov, and A. K. Geim, *Proc. Natl. Acad. Sci. U.S.A.* **102**, 10451 (2005).
- ³ A. K. Geim and K. S. Novoselov, *Nature Materials* **6**, 183 (2007).
- ⁴ A. H. Castro Neto, F. Guinea, N. M. R. Peres, K. S. Novoselov, and A. K. Geim, *Rev. Mod. Phys.* **81**, 109 (2009).
- ⁵ G. Li, A. Luican, and E. Y. Andrei, *Phys. Rev. Lett.* **102**, 176804 (2009).
- ⁶ Y. Zhang, V. W. Brar, F. Wang, C. Girit, Y. Yayon, M. Panlasigui, A. Zettl, and M. F. Crommie, *Nature Phys.* **4**, 627 (2008).
- ⁷ T. O. Wehling, I. Grigorenko, A. I. Lichtenstein, and A. V. Balatsky, *Phys. Rev. Lett.* **101**, 216803 (2008).
- ⁸ A. L. Vázquez de Parga, F. Calleja, B. Borca, M. C. Passeggi, J. J. Hinarejos, F. Guinea, and R. Miranda, *Phys. Rev. Lett.* **100**, 056807 (2008).
- ⁹ B. Borca, S. Barja, M. Garnica, M. Minniti, A. Politano, J. M. Rodríguez-García, J. J. Hinarejos, Daniel Farías, A. L. Vázquez de Parga, and R. Miranda (2010), arXiv:1005.1764.
- ¹⁰ C. Oshima and A. Nagashima, *J. Phys. Condens. Matter* **9**, 1 (1997).
- ¹¹ A. T. NDiaye, S. Bleikamp, P. J. Feibelman, and T. Michely, *Phys. Rev. Lett.* **97**, 215501 (2006).
- ¹² S. Marchini, S. Günther, and J. Wintterlin, *Phys. Rev. B* **76**, 075429 (2007).
- ¹³ D. Martocchia, P. R. Willmott, T. Brugger, M. Björck, S. Günther, C. M. Schlepütz, A. Crevellino, S. A. Pauli, B. D. Patterson, S. Marchini, et al., *Phys. Rev. Lett.* **101**, 126102 (2008).
- ¹⁴ Y. Pan, N. Jiang, J. T. Sun, D. X. Shi, S. X. Du, F. Liu, and H.-J. Gao, *Adv. Mat.* **20**, 1 (2008).
- ¹⁵ D.-E. Jiang, M.-H. Du, and S. Dai (2008), arXiv:0901.1101.
- ¹⁶ D. Usachov, A. M. Dobrotvorskii, A. Varykhalov, O. Rader, W. Gudat, A. M. Shikin, and V. K. Adamchuk, *Phys. Rev. B* **78**, 085403 (2008).
- ¹⁷ S. Y. Zhou, G.-H. Gweon, A. V. Fedorov, P. N. First, W. A. de Heer, D.-H. Lee, F. Guinea, A. Neto, and A. Lanzara, *Nature Materials* **6**, 770 (2007).
- ¹⁸ C.-H. Park, L. Yang, Y.-W. Son, M. L. Cohen, and S. G. Louie, *Nature Physics* **4**, 213 (2008).
- ¹⁹ C.-H. Park, L. Yang, Y.-W. Son, M. L. Cohen, and S. G. Louie, *Phys. Rev. Lett.* **101**, 126804 (2008).
- ²⁰ R. P. Tiwari and D. Stroud, *Phys. Rev. B* **79**, 205435 (2009).
- ²¹ L. Brey and H. A. Fertig, *Phys. Rev. Lett.* **103**, 046809 (2009).
- ²² M. Barbier, P. Vasilopoulos, and F. M. Peeters (2010), arXiv:1002.1442v1.
- ²³ D. P. Arovas, L. Brey, H. A. Fertig, E.-A. Kim, and K. Ziegler (2010), arXiv:1002.3655.
- ²⁴ I. Snyman, *Phys. Rev. B* **80**, 054303 (2009).
- ²⁵ Y. P. Bliokh, V. Freilikher, S. Savel'ev, and F. Nori, *Phys. Rev. B* **79**, 075123 (2009).
- ²⁶ N. Abedpour, A. Esmailpour, R. Asgari, and M. R. Tabar, *Phys. Rev. B* **79**, 165412 (2009).
- ²⁷ A. V. Shytov, D. A. Abanin, and L. S. Levitov, *Phys. Rev. Lett.* **103**, 016806 (2009).
- ²⁸ M. Gibertini, A. Singha, V. Pellegrini, M. Polini, G. Vignale, A. Pinczuk, L. N. Pfeiffer, and K. W. West, *Phys. Rev. B* **79**, 241406 (2009).
- ²⁹ L. Rosales, M. Pacheco, Z. Barticevic, A. León, A. Latgé, and P. A. Orellana, *Phys. Rev. B* **80**, 073402 (2009).
- ³⁰ F. Guinea, M. I. Katsnelson, and A. K. Geim, *Nature Phys.* **6**, 30 (2010).
- ³¹ C.-H. Park, Y.-W. Son, L. Yang, M. L. Cohen, and S. G. Louie, *Phys. Rev. Lett.* **103**, 046808 (2009).
- ³² J. da Silva-Araújo, H. Chacham, and R. W. Nunes, *Phys. Rev. B* **81**, 193405 (2010).
- ³³ J. L. Mañes, F. Guinea, and M. A. H. Vozmediano, *Phys. Rev. B* **75**, 155424 (2007).
- ³⁴ M. A. H. Vozmediano, M. I. Katsnelson, and F. Guinea (2010), arXiv:1003.5179.
- ³⁵ F. Guinea, B. Horovitz, and P. L. Doussal, *Phys. Rev. B* **77**, 205421 (2008).
- ³⁶ F. D. M. Haldane, *Phys. Rev. Lett.* **61**, 2015 (1988).